CrossMark

ORIGINAL PAPER

3D-Dixon MRI based volumetry of peri- and epicardial fat

Rami Homsi[1] · Michael Meier-Schroers[1] · Jürgen Gieseke[1,2] · Darius Dabir[1] ·
Julian A. Luetkens[1] · Daniel L. Kuetting[1] · Claas P. Naehle[1,2,3] · Christian Marx[1] ·
Hans H. Schild[1] · Daniel K. Thomas[1] · Alois M. Sprinkart[1,3]

Abstract There is growing evidence that pericardial and epicardial fat volume (PFV, EFV) are associated with cardiovascular risk. We evaluated a novel method for accurate measurement of PFV and EFV using a 3D-Dixon based cardiac magnetic resonance (CMR) approach. An electrocardiography triggered and respiratory navigator gated 3D-gradient echo pulse sequence was used for cardiac Dixon imaging. Based on this sequence, voxels predominantly containing fat were identified and added up for volumetry. After accuracy assessment in phantoms, consisting of muscle tissue and seven different fat samples (50–200 ml), the sequence was acquired in 34 healthy volunteers (22 male, BMI range 14–42 kg/m^2, age range 21–79 years) at 1.5 T. Analysis was performed independently by two readers who draw two 3D-regions of interest, one for EFV and one for PFV. Additionally, EFV and PFV were compared between overweighted and non-overweighted subjects. The phantom study showed an excellent agreement of measured and true fat volumes (maximum difference = 6 %, linear correlation coefficient R = 1.00). PFV over all volunteers was 158.0 ± 126.4 ml and EFV was 77.0 ± 55.3 ml. PFV and EFV were highly correlated (R = 0.96). Inter-reader agreement was good with a mean difference of 0.2 ± 5.6 and 4.5 ± 4.2 ml for PFV/EFV, (R > 0.99, each). EFV and PFV differed significantly between subjects with BMI > 25 kg/m^2 and BMI < 25 kg/m^2, n = 17 each (PFV 219.0 ± 151.8 vs. 96.9 ± 44.7 ml and EFV 102.3 ± 66.3 vs. 51.7 ± 23.6 ml, $p < 0.001$, each). The proposed 3D-Dixon based method allows accurate measurement of cardiac fat volumes. It provides a valuable tool for cardiovascular risk stratification by CMR.

Keywords CMR · Epicardial fat · Pericardial fat · Volumetry · Dixon

Introduction

Cardiac magnetic resonance (CMR) is increasingly used to assess cardiovascular risk, and to diagnose cardiovascular diseases, which are a leading cause of mortality and morbidity [1]. One parameter which has been associated with cardiovascular risk and disease is the volume of epicardial and pericardial adipose tissue [2, 3]. The epicardial adipose tissue is the fat tissue adjoining the myocardium which is covered by the pericardium. The pericardial adipose tissue refers to the whole amount of mediastinal fat including the epicardial adipose tissue as well as the extra pericardial fat surrounding the heart [2, 3]. Besides serving as an energy storage and mechanical protection, recent studies suggest that fatty tissue is also endocrine/metabolically active [4, 5]. Epicardial and pericardial adipose tissue, e.g. measured as epicardial and pericardial fat volume (EFV and PFV), have been shown to be associated with different cardiovascular diseases or cardiovascular risk factors, such as coronary atherosclerosis, myocardial ischemia, left ventricular (LV) dysfunction, and diabetes mellitus [3, 5, 6], and their measurement has gained increased attention in the last years.

✉ Alois M. Sprinkart
  martin.sprinkart@ukb.uni-bonn.de

[1] Department of Radiology, University of Bonn, Sigmund-Freud-Str. 25, 53127 Bonn, Germany

[2] Philips Healthcare Germany, Lübeckertordamm, Hamburg, Germany

[3] Institute of Medical Engineering, Ruhr-University Bochum, Universitätsstraße, Bochum, Germany

In magnetic resonance imaging (MRI), the chemical shift between protons in water and protons in fat can be exploited to separate the signal from fat and water, which allows reconstruction of water-only images, fat-only images [7, 8] and the computation of fat-fraction maps. Therefore CMR has the potential to provide accurate measurements of PFV and EFV. However, to the best of our knowledge up to date no studies have been performed implementing such a technique to measure PFV and EFV in a three-dimensional volumetric approach. Therefore, the purpose of this study was to implement an electrocardiography (ECG)-triggered and respiratory gated 3D-Dixon [7–9] pulse sequence along with an appropriate post-processing approach and investigating its suitability for cardiac fat volume measurements with phantom study validation. Additionally, healthy individuals were investigated to evaluate EFV and PFV using the proposed method and to correlate these parameters with physiologic parameters like body mass index (BMI) and age.

Materials and methods

The study protocol was approved by the local ethic committee. All scans were performed on a 1.5 Tesla (T) MR system (Ingenia, Philips Healthcare, Best, The Netherlands) with a maximum gradient strength of 45 mT/m and a maximum slew rate of 120 mT/m/ms. A 32 channel torso coil with digital interface was used for signal reception.

Phantom validation

To test the accuracy of the proposed fat volume measurement, phantoms simulating the coexistence of muscle and fatty tissue were built. Seven different samples of warmed-up lard (50–200 ml) were measured with a syringe and filled into a box so that low fat pork was surrounded by fat (Fig. 1). After construction of the phantoms, fat volumes were determined similar to the in vivo measurements described below. The same sequence settings were used for phantom and in vivo exams.

Study population

34 healthy subjects (12 women, 22 men) with a wide range of BMI (14–42 kg/m^2, 25.4 ± 5.3 kg/m^2 (mean ± standard deviation)) and age (21–79 years, 42.2 ± 14.9 years) were examined. Subjects had no known medical conditions or history of cardiac disease. Written informed consent was obtained from all study subjects prior to CMR. Exclusion criteria included contraindications for CMR and any evidence of cardiovascular pathologies. Further cardiac

characteristics of the study participants can be found in Table 1.

MRI acquisition

Functional imaging

ECG-gated SSFP-cine images were obtained in breath-hold in the horizontal long axis, the vertical long axis, left ventricular outflow tract, and short axis for wall motion and functional analysis. Sequence parameters were as follows: field of view (FOV) = 350 × 350 mm^2, slice thickness = 8 mm, pixel size = 1.7 × 1.7 mm^2, reconstructed to 1 × 1 mm^2, repetition time (TR) = 3.1 ms, echo time (TE) = 1.6 ms, flip angle (α) = 60°, parallel imaging factor (SENSE) = 2.5, number of cardiac phases reconstructed = 40.

Dixon chemical shift imaging

For assessment of epi- and pericardial fat volumes, a 3D transversal ECG-triggered and respiratory navigator gated magnetization prepared mDixon-sequence [10] was acquired. The "gate and track" option of the scanner software was used, i.e. navigator gating was combined with prospective motion correction [11]. Trigger delay was set to end-diastole and optimized by means of cine MRI data. The following sequence parameters were used: FOV = 350 × 302 × 180 mm^3; voxel size = 1.5 × 1.5 × 3.0 mm^3 (120 overcontiguous slices), reconstructed voxel size = 1.0 × 1.0 × 1.5 mm^3, TR = 5.4 ms, TE$_1$/TE$_2$ = 1.8 ms/4.0 ms; α = 20°, parallel imaging factor (SENSE) = 1.5 in both phase encoding directions, water fat shift = 0.16 pixel, arrhythmia rejection was applied, T2 preparation = 50 ms, acquisition window = 100–156 ms (selected based on cine MRI data). In-phase (IP), opposed-phase (OP), water only (W), and fat only (F) images were reconstructed online at the scanner console using an algorithm described in [8].

Image analysis

Cardiac parameters

Left ventricular end systolic (LVESV) and end diastolic volume (LVEDV) were determined offline based on the volumetric assessment of the cine sequences in the short axis orientation using dedicated software (ViewForum, Philips Healthcare) by manual tracing of the endocardial borders. Papillary muscles were included in the left ventricular cavity volume. Left ventricular function was assessed in all subjects by computation of the ejection fraction (LVEF) using the formula (LVEDV–LVESV)/
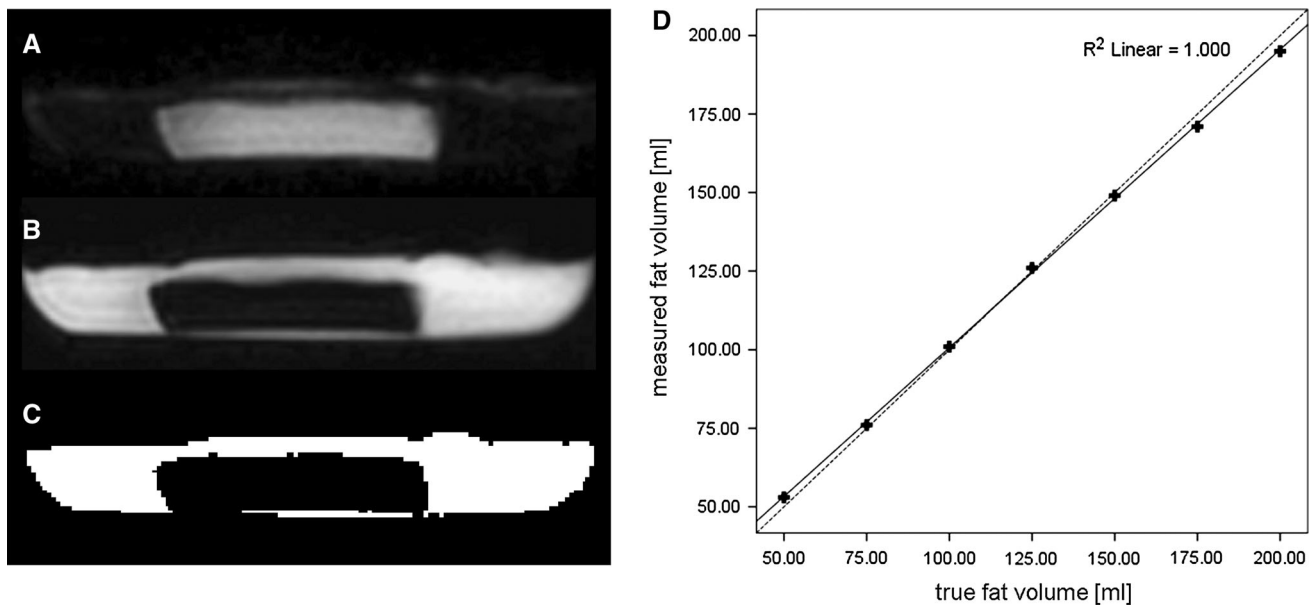
Fig. 1 Phantom study: The phantoms were constructed of low-fat pork surrounded by lard. The pork/muscle appears hyperintense in the reconstructed transversal water image (a) and hypointense on the fat only image (b). Image (c) shows the result of the segmentation of voxels predominantly containing fat after determination and application of an appropriate threshold in the fat-fraction map. In total, seven of such phantoms with fat volumes from 50 to 200 ml were build. The diagram (d) shows the accuracy of the fat volume measurements in the phantom study. The *dashed line* equals unity and represents perfect agreement between measured and true fat volumes

Table 1 In-vivo fat volume measurements and cardiac characteristics: Results are given as mean $\pm$ standard deviation

	All (n = 34)	BMI < 25 kg/m^2 (n = 17)	BMI > 25 kg/m^2 (n = 17)	p for difference between BMI groups
Age (years)	42.2 $\pm$ 14.9	42.9 $\pm$ 16.0	41.4 $\pm$ 14.3	0.76
Heart rate (beats per minute)	69.6 $\pm$ 12.2	72.3 $\pm$ 12.7	66.9 $\pm$ 11.4	0.21
LV ejection fraction (%)	63.6 $\pm$ 6.0	63.2 $\pm$ 5.8	63.9 $\pm$ 6.3	0.74
LV end diastolic volume/BSA (ml/m^2)	74.2 $\pm$ 13.1	72.1 $\pm$ 13.8	76.3 $\pm$ 12.3	0.36
PFV (ml)	158.0 $\pm$ 126.4	96.9 $\pm$ 44.7	219.0 $\pm$ 151.8	**<0.01**
PFV/BSA (ml/m^2)	78.2 $\pm$ 54.8	52.4 $\pm$ 21.6	104.0 $\pm$ 65.7	**<0.01**
EFV (ml)	77.0 $\pm$ 55.3	51.7 $\pm$ 23.6	102.3 $\pm$ 66.3	**<0.01**
EFV/BSA (ml/m^2)	38.5 $\pm$ 24.3	28.0 $\pm$ 11.3	48.9 $\pm$ 29.3	**<0.01**

PFV/EFV pericardial/epicardial fat volume, *BSA* body surface area, *BMI* body mass index, *LV* left ventricle

LVEDV $\times$ 100. LVEF was compared between the two BMI groups and correlation with fat volumes was analyzed.

PFV and EFV measurement

Dixon Images were analyzed offline on a personal computer using in-house software written in MATLAB (The MathWorks, Inc., Natick, MA). PFV and EFV were measured between the bifurcation of the pulmonary artery to the most inferior transversal slice of the myocardium [2].

Two regions of interest (ROI) were drawn per slice. The first ROI contours the pericardial border. The second ROI includes all pericardial fatty tissue. To identify voxels predominantly containing fat, a fat-fraction (FF) map was computed based on the fat- and water-only images, with $FF = F/(F + W)$. Since the dual-echo mDixon sequence was primarily optimized for image quality aspects rather than for direct quantification of the proton density fat fraction, the signal of fat and water is weighted by T1, T2 and T2* relaxation effects [12]. This means that a value of 0.5 in the FF map does not correspond to a voxel with 50 % fat and 50 % water. Therefore, to determine an appropriate threshold in the FF map for the segmentation of voxels predominantly containing fat, the magnitude of the signal of pure fat voxels (S_{fat}) and the signal of myocardium (S_{myo}) was determined in all subjects, and the threshold was set to $FF_{thresh} = S_{fat}/(S_{fat} + S_{myo})$. To avoid a

potential influence of spatial varying transmit coil sensitivities or residual spatial signal inhomogeneities that might appear in case of suboptimal body coil normalization, the corresponding fat and myocardial ROIs were placed in close proximity of each other. In contrast to the calculation of a threshold based on the sequence signal model, this straight forward approach is independent of particular sequence settings. Additionally it should potentially also work at a field strength of 3 T and doesn't require the knowledge of tissue relaxation times. This is particularly of benefit, if fat volumetry is performed based on a high-resolution Dixon sequence for contrast enhanced coronary angiography [10]. Moreover, an appropriate noise threshold was applied by including only voxels in the analyses with signal intensities higher than that of the erector spinae muscle. With the applied sequence settings the signal intensity of the erector spinae muscle is approximately 25 % of pure fat voxels which is high enough to suppress voxels in the lung and low enough to prevent exclusion of relevant voxels containing peri- od epicardial fat. Finally, peri- and epicardial fat volumes were determined by multiplying the number of fat voxels inside the three-dimensional ROIs by the voxel size [13]. All post-processing steps were summarized in Fig. 2. PFV and EFV were additionally normalized to the body surface area. Body surface area (BSA) was estimated from height and weight [14].

For assessment of the inter-reader agreement, two observers with more than 2 years of experience in CMR, independently performed the PFV and EFV measurements.

Measurement of epi- and pericardial fat areas and right ventricular epicardial fat thickness

Based on the SSFP cine images we performed measurements of epicardial fat thickness (EFT) and peri- and epicardial fat area (PFA and EFA) for comparison with 3D-Dixon volumetric measurements. EFT measurements were performed at the right ventricle free wall in systole [15, 16]. EFA and PFA were assessed in the horizontal long axis view in diastole [17, 18]. To evaluate the feasibility of reliable estimation of fat volumes based on the obtained 1D and 2D measurements, EFV/PFV was predicted based on the EFT, EFA, and PFA measures applying a linear model.

Statistical analysis

All statistical analyses were performed in SPSS, (IBM SPSS Statistics 22.0, Armonk, New York). Study participant characteristics are presented as mean ± standard deviation or as absolute frequency. The unpaired Student t test was used for comparison of continuous variables between the two groups. Linear regression analysis was
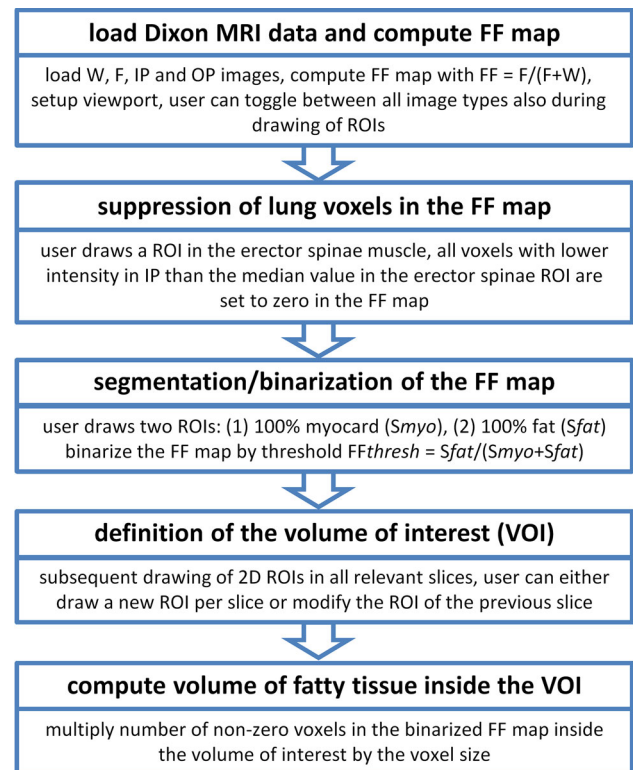

Fig. 2 Post-processing steps for volumetry of epi- and pericardial fat based on Dixon MRI images: the last two steps are performed twice, once for the determination of the epicardial fat volume, once for the pericardial fat volume

performed for comparison of two continuous variables. Multi-comparisons were performed using an analysis of covariance (ANCOVA). The level of significance was set to 0.05. A Bland–Altman analysis was performed for assessment of inter-observer agreement.

Results

Measurements in the fat-muscle phantoms showed a very good agreement of measured and true fat volume (maximum difference = 6 %) with an excellent correlation between measured fat volumes and true fat volumes (linear correlation coefficient R = 1.00), see Fig. 1.

In the in vivo study, a total number of 34 volunteers were enrolled with a wide range of age and BMI. The in-vivo net scan duration of the mDixon sequence was 3–5 min. With an assumed navigator efficiency of 40–50 %, the total acquisition time was on average about 7.5 min. The total time for offline analyses for both epi- and pericardial fat volume measurements was 12–15 min.

The 3D-Dixon sequence allowed a reliable separation of fat and water with an image quality that allowed manual tracing of the pericardial border in all subjects (Figs. 3 and 4). The
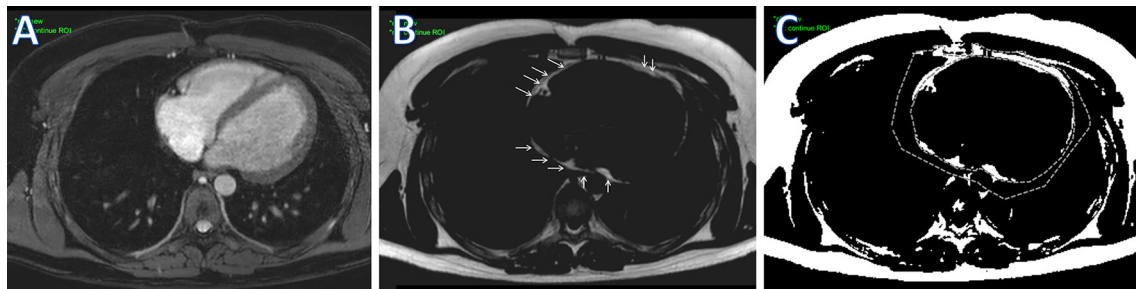
Fig. 3 Dixon image analysis for measurement of pericardial and epicardial fat volume (PFV and EFV) in a 21 year old healthy male: Image A shows the water only image, image B the fat only image. The arrows point at the contour of the pericardial outline, which corresponds to the region of interest (ROI) for the measurement of the EFV. In C, the regions of interest were transferred to the image of the segmented fat voxels. The dashed lines mark the ROIs for measurement of EFV (inner) and PFV, respectively

Fig. 4 Fat only images in a 69 year old female from cranial to caudal (**a–c**). The pericardial outline (*arrows*) could be identified at all slice locations

determined fat fraction threshold was 0.74 ± 0.02. Results of the fat volume measurements are shown in Table 1. A high linear correlation was observed between pericardial and epicardial fat volumes (R = 0.96, see Fig. 5) and also between (PFV-EFV) and EFV (R = 0.89). No significant correlations were found between fat volumes and heart rate ($p > 0.2$, each) or fat volumes and left ventricular ejection fraction ($p > 0.2$, each).

The Bland–Altman analysis for inter-observer agreement revealed a good agreement between the results of cardiac fat volume measurements performed by two different readers. Mean differences between the observers were 0.2 ml with 95 % limits of agreement (LoA) of (−10.7; 11.2) ml for the pericardial fat volume (linear correlation coefficient R = 0.999) and 4.5 ml with 95 % LoA of (−3.8; 12.7) (R = 0.998) for epicardial fat volume measurements.

By splitting the study population into two groups with group A: BMI < 25 kg/m^2 and group B: BMI > 25 kg/m^2, a significant difference in peri- as well as epicardial fat volumes between overweighted and non-overweighted subjects was observed (Table 1). There was no significant difference in age between the two groups. Figure 6 shows the scatterplot for the association between BMI and the determined fat volumes. An analysis of covariance with fat volumes as the dependent variable and BMI and age as independent variables underlined the association between BMI and cardiac fat volumes ($p < 0.001$, for PFV and EFV). The association between cardiac fat volumes and age was also statistically significant ($p = 0.02$ for PFV and $p = 0.04$ for EFV) with an increase in fat volumes at higher age.

The comparison of 1D, 2D and 3D measures of cardiac fat deposits are shown in Fig. 7. A highly significant linear correlation was observed between EFT and EFV, EFA and EFV, and PFA and PFV ($p < 0.005$, each). However, when the individual fat volumes are predicted based on 1D and 2D measurements, large deviations from the volume measurements were observed. With a linear model, differences between measured and predicted values were on average 47 % (median 36 %, range 1–280 %) for EFT/EFV, 40 % (median 27 %, 1–288 %) for EFA/EFV, and 38 % (median 24 %, range 1–244 %) for PFA/PFV.

Discussion

An association between cardiovascular risk and cardiac fat has been described [2–5]. The speculated underlying mechanism is the production of metabolically and inflammatory bioactive molecules by cardiac adipose tissue [4, 5, 19, 20]. Therefore the measurement of epicardial and pericardial fat volumes is an important step in cardiovascular risk stratification.
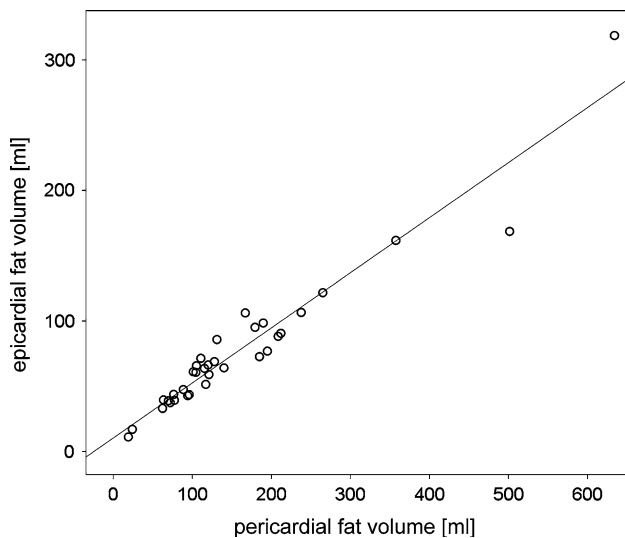
Fig. 5 Scatterplot for epicardial fat volume and pericardial fat volume demonstrating the association between both measures
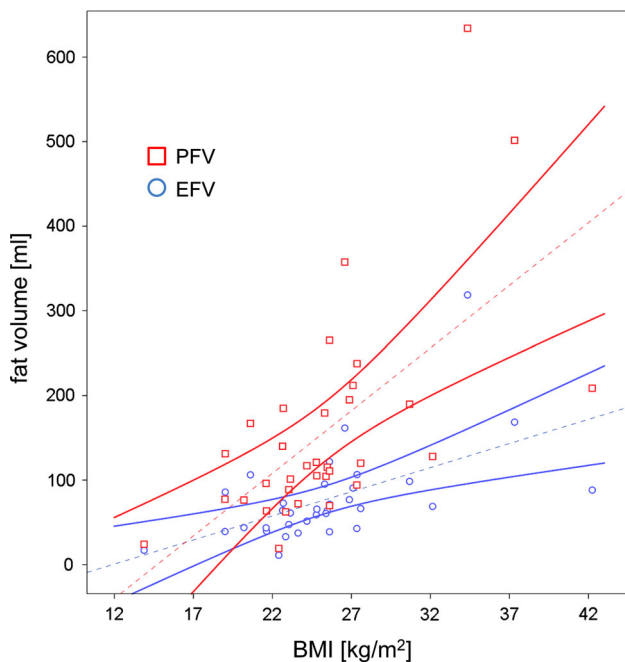

Fig. 6 Scatterplot for determined fat volumes (PFV: *red squares*, EFV: *blue circles*) and BMI: Despite huge inter-individual variations, a clear association between cardiac fat volumes and BMI could be observed. The *red* and the *blue curves* define the 95 % confidence interval of the mean for PFV and EFV, respectively

For the first time an ECG-triggered and respiratory navigator gated 3D mDixon sequence was employed for the measurement of epi- and pericardial fat volume in healthy volunteers. The Dixon method is ideally suited for such an approach because it offers a robust separation of water and fat and it is relatively insensitive to inhomogeneities of the static magnetic field [7–10, 21]. However,

a segmentation of fat tissue based on a simple signal threshold in the fat only image is problematic, as results are extremely susceptible to little variations of the applied threshold. By identification of voxels predominantly containing fat based on the relative signal contribution of fat per voxel allowed accurate measurements of the fat volume as demonstrated in the phantom study. However, relaxation effects have to be accounted for in order to obtain valid quantitative results [21].

Image quality was sufficient to allow detection of the pericardial outlines, as confirmed by the low inter-observer variability for PFV and EFV. Hence, the amount of epi- and pericardial fat could be accurately quantified separately. This may be of importance, since particularly epicardial adipose tissue, which stems from another cell line during embryogenesis than adipose tissue outside the pericardium [3, 24, 25], has been shown to have high lipogenic and lipolytic activity [22, 23]. However, in our study we found a strong correlation between EFV and PFV. This raises the question whether separating both pools is necessary, as a single measurement of PFV only would be significantly more time efficient. Currently it is still under debate which of the two pools is more important as a marker for cardiovascular risk [10] so that further detailed studies in patients are necessary to answer this question.

In general, the evaluation of epi- and pericardial fat using CMR is not yet widely applied and up to date only few CMR studies with small patient samples have been published. The different methods described include the simple measurement of the epicardial fat thickness at the right ventricular free wall analogous to transthoracic echocardiography (TTE) [26], the volumetric measurements using the modified Simpson method in a defined location—such as around the ventricles—by identification of the contours of adipose tissue with e.g. steady state free precession (SSFP) or black blood sequences [26, 27], and 2D measurements of fat areas e.g. in a horizontal long axis slice [17, 18]. No MRI method has been introduced which measures the volumes of epi- and pericardial fat by a 3D-segmentation of voxels that predominantly contain fat, similar to ECG-gated cardiac computer tomography with at least 16 detector rows (CT) [2, 20, 28, 29]. In CT, the differences between the Hounsfield units of fat (HU = −30 to −190) and other tissue is used to identify and measure cardiac fat volumes [2, 20, 29, 30]. Similar to CT, our volume measurements were performed in diastole and also showed a low inter-observer variability [31, 32]. However, the most easy and rapid way to assess epicardial fat is by measurement of the epicardial fat thickness using TTE [33]. Here, the hypoechoic space between the epicardial surface and the parietal pericardium at the region of the right ventricular free wall is measured. Mean systolic thickness was described to range between 6.5 mm and
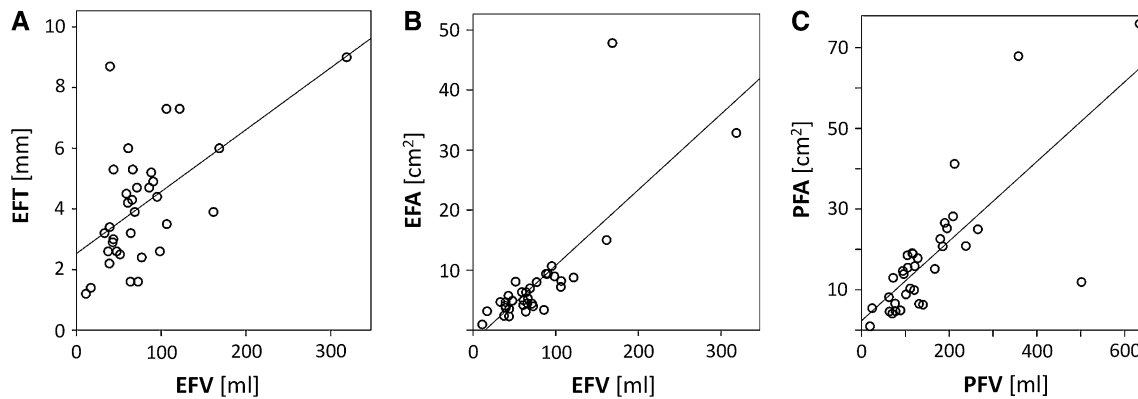
Fig. 7 Comparison of 1D, 2D and 3D measurements of cardiac fat deposits: The scatterplots display the association between the epicardial fat volume (EFV) and the measurement of the epicardial fat thickness (EFT) at the right ventricular free wall (**a**), between EFV and the epicardial fat area (EFA) in the horizontal long axis view (**b**), and between the pericardial fat volume (PFV) and the pericardial fat area (PFA) (**c**). A linear model based on regression analyses of these data was used to predict EFV and PFV from the respective 1D and 2D data (see text for results)

7.6 mm [15, 16] and diastolic thickness between 3.2 and 6.4 mm [16, 34]. TTE has several disadvantages, such as a possible confusion with pericardial fluid and that pericardial fat amounts cannot be evaluated. Also, it is still controversial if measurements should be taken in systole or in diastole, as different diameters do result [35, 36]. Furthermore inter-observer variations may be higher than in a volumetric assessment [31–33] due to an observer related image quality and differences in echocardiography windows, as only a diameter is measured at a single anatomic location.

Our 1D and 2D measurements performed analog to previous work, e.g. [15, 16] and [17, 18], show statistically significant linear correlations between the determined fat volumes and the respective 1D and 2D measures. However, reliable estimates of the individual cardiac fat volumes are not feasible. Compared to a real volumetric approach, the determination of only 1D or 2D measures may thus reduce the statistical power in cardiac studies and eventually may under- or overestimate the cardiovascular risk in the individual case. In contrast, 3D-Dixon offers the advantage of a three-dimensional volumetric approach similar to CT without necessitating radiation exposure. A further advantage is the possibility to accurately separate epi- and pericardial fat, which sometimes can be difficult in CT [37], and which is not possible with TTE [15, 16]. Furthermore, even the amount of fat in the most apical slices can be quantified with the proposed approach which may be relevant, since the amount of fat in this area can vary significantly and is missed by 1D and 2D approaches. Our CMR derived data revealed a mean value for EFV of 77.0 ± 55.3 ml over the whole population; mean volumes measured with CT for EFV are similar varying in literature from 68 to 137 ml [20, 29]. The results for correlation of EFV and PFV with BMI and age are in concordance with previous studies [15, 20, 31, 38]. Larger fat volumes were observed in subjects with higher BMI [15, 20] and older subjects have more epicardial and pericardial adipose tissue compared to younger subjects [38], which may be explained by loss of lean body mass with increase in fat mass and redistribution to the trunk and viscera [39].

Finally, the T2 prepared mDixon sequence is potentially helpful in evaluating additional findings due to its predominant T2-weighting and the fat-only and fat-free images. This may allow for assessment of mediastinal, cardiac or even liver masses and also the proximal coronary arteries. Though, for a more extensive evaluation of the coronary arteries a higher spatial resolution is required allowing both accurate fat volume measurement and coronary MR angiography by acquisition of a single sequence [10].

Our study has several limitations. First, a relatively long acquisition window was used in the healthy volunteers ranging from 100 to 156 ms. Especially in patients with high heart rates it may be mandatory to select a shorter shot duration in order to avoid motion artifacts. Second, the method was only validated in a phantom study due to the lack of an in vivo reference standard. Results were only compared to other CT studies. Since CT requires the application of ionizing radiation it was not possible to perform an intra-subject comparison in healthy volunteers without clear indication for a CT examination. Third, the low number of subjects examined in this study is also a limitation. However, the inclusion of healthy subjects with a wide range of BMI and age allowed for evaluation of the association between different risk factors.

In conclusion, using the implemented Dixon method PFV as well as EFV can be measured with a three-dimensional approach analogous to CT, but without the need of ionizing radiation. Therefore this approach is ideally

suited for future studies of PFV and EFV and its role in cardiovascular risk stratification and disease.

Compliance with ethical standards

Conflict of interest All authors declare that they have no conflict of interest.

Ethical approval All procedures performed in studies involving human participants were in accordance with the ethical standards of the institutional research committee and with the 1964 Helsinki declaration and its later amendments or comparable ethical standards.

Informed consent Informed consent was obtained from all individual participants included in the study.

References

1. World Health Organization (2013) Cardiovascular diseases. World Health Organization, Switzerland, Fact Sheet 317
2. Dey D, Nakazato R, Li D, Berman DS (2012) Epicardial and thoracic fat—noninvasive measurement and clinical implications. Cardiovasc Diagn Ther 2(2):85–93
3. Sacks HS, Fain JN (2007) Human epicardial adipose tissue: a review. Am Heart J 153(6):907–917
4. Iacobellis G, Corradi D, Sharma AM (2005) Epicardial adipose tissue: anatomic, biomolecular and clinical relationships with the heart. Nat Clin Pract Cardiovasc Med 2(10):536–543
5. Iacobellis G, Pistilli D, Gucciardo M et al (2005) Adiponectin expression in human epicardial adipose tissue in vivo is lower in patients with coronary artery disease. Cytokine 29(6):251–255
6. Yong HS, Kim EJ, Seo HS et al (2010) Pericardial fat is more abundant in patients with coronary atherosclerosis and even in the non-obese patients: evaluation with cardiac CT angiography. Int J Cardiovasc Imaging 26(Suppl 1):53–62
7. Dixon WT (1984) Simple proton spectroscopic imaging. Radiology 153(1):189–194
8. Eggers H, Brendel B, Duijndam A, Herigault G (2011) Dual-echo Dixon imaging with flexible choice of echo times. Magn Reson Med 65(1):96–107
9. Yu H, Reeder SB, Shimakawa A, Brittain JH, Pelc NJ (2005) Field map estimation with a region growing scheme for iterative 3-point water-fat decomposition. Magn Reson Med 54(4):1032–1039
10. Bornert P, Koken P, Nehrke K, Eggers H, Ostendorf P (2014) Water/fat-resolved whole-heart Dixon coronary MRA: an initial comparison. Magn Reson Med 71(1):156–163
11. McConnell MV, Khasgiwala VC, Savord BJ et al (1997) Prospective adaptive navigator correction for breath-hold MR coronary angiography. Magn Reson Med 37(1):148–152
12. Liu CY, Redheuil A, Ouwerkerk R, Lima JA, Bluemke DA (2010) Myocardial fat quantification in humans: evaluation by two-point water-fat imaging and localized proton spectroscopy. Magn Reson Med 63(4):892–901
13. Brennan DD, Whelan PF, Robinson K et al (2005) Rapid automated measurement of body fat distribution from whole-body MRI. AJR Am J Roentgenol 185(2):418–423
14. DuBois D, DuBois EF (1916) Clinical calorimetry: tenth paper: A formula to estimate the approximate surface area if height and weight be known. Arch Intern Med (Chic) XVII(6_2):863–871
15. Iacobellis G, Willens HJ, Barbaro G, Sharma AM (2008) Threshold values of high-risk echocardiographic epicardial fat thickness. Obesity (Silver Spring) 16(4):887–892
16. Jeong JW, Jeong MH, Yun KH et al (2007) Echocardiographic epicardial fat thickness and coronary artery disease. Circ J 71(4):536–539
17. Nyman K, Graner M, Pentikainen MO et al (2013) Cardiac steatosis and left ventricular function in men with metabolic syndrome. J Cardiovasc Magn Reson 15:103
18. Graner M, Siren R, Nyman K et al (2013) Cardiac steatosis associates with visceral obesity in nondiabetic obese men. J Clin Endocrinol Metab 98(3):1189–1197
19. Mazurek T, Zhang L, Zalewski A et al (2003) Human epicardial adipose tissue is a source of inflammatory mediators. Circulation 108(20):2460–2466
20. Rosito GA, Massaro JM, Hoffmann U et al (2008) Pericardial fat, visceral abdominal fat, cardiovascular disease risk factors, and vascular calcification in a community-based sample: the Framingham heart study. Circulation 117(5):605–613
21. Kukuk GM, Hittatiya K, Sprinkart AM et al (2015) Comparison between modified Dixon MRI techniques, MR spectroscopic relaxometry, and different histologic quantification methods in the assessment of hepatic steatosis. Eur Radiol 25(10):2869–2879
22. Corradi D, Maestri R, Callegari S et al (2004) The ventricular epicardial fat is related to the myocardial mass in normal, ischemic and hypertrophic hearts. Cardiovasc Pathol 13(6):313–316
23. Marchington JM, Pond CM (1990) Site-specific properties of pericardial and epicardial adipose tissue: the effects of insulin and high-fat feeding on lipogenesis and the incorporation of fatty acids in vitro. Int J Obes 14(12):1013–1022
24. Talman AH, Psaltis PJ, Cameron JD, Meredith IT, Seneviratne SK, Wong DT (2014) Epicardial adipose tissue: far more than a fat depot. Cardiovasc Diagn Ther 4(6):416–429
25. Marchington JM, Mattacks CA, Pond CM (1989) Adipose tissue in the mammalian heart and pericardium: structure, foetal development and biochemical properties. Comp Biochem Physiol B Comp Biochem 94(2):225–232
26. Fluchter S, Haghi D, Dinter D et al (2007) Volumetric assessment of epicardial adipose tissue with cardiovascular magnetic resonance imaging. Obesity (Silver Spring) 15(4):870–878
27. Hua N, Chen Z, Phinikaridou A et al (2014) The influence of pericardial fat upon left ventricular function in obese females: evidence of a site-specific effect. J Cardiovasc Magn Reson 16:37
28. Elming MB, Lonborg J, Rasmussen T et al (2013) Measurements of pericardial adipose tissue using contrast enhanced cardiac multidetector computed tomography–comparison with cardiac magnetic resonance imaging. Int J Cardiovasc Imaging 29(6):1401–1407
29. Dey D, Suzuki Y, Suzuki S et al (2008) Automated quantitation of pericardiac fat from noncontrast CT. Invest Radiol 43(2):145–153
30. Yoshizumi T, Nakamura T, Yamane M et al (1999) Abdominal fat: standardized technique for measurement at CT. Radiology 211(1):283–286
31. Gorter PM, de Vos AM, van der Graaf Y et al (2008) Relation of epicardial and pericoronary fat to coronary atherosclerosis and coronary artery calcium in patients undergoing coronary angiography. Am J Cardiol 102(4):380–385
32. Nakazato R, Shmilovich H, Tamarappoo BK et al (2011) Interscan reproducibility of computer-aided epicardial and thoracic fat measurement from noncontrast cardiac CT. J Cardiovasc Comput Tomogr 5(3):172–179
33. Iacobellis G, Assael F, Ribaudo MC et al (2003) Epicardial fat from echocardiography: a new method for visceral adipose tissue prediction. Obes Res 11(2):304–310
34. Ahn SG, Lim HS, Joe DY et al (2008) Relationship of epicardial adipose tissue by echocardiography to coronary artery disease. Heart 94(3):e7

35. Mookadam F, Goel R, Alharthi MS, Jiamsripong P, Cha S (2010) Epicardial fat and its association with cardiovascular risk: a cross-sectional observational study. Heart Views 11(3):103–108

36. Iacobellis G, Willens HJ (2009) Echocardiographic epicardial fat: a review of research and clinical applications. J Am Soc Echocardiogr 22(12):1311–1319; quiz 1417–1318

37. Ding J, Hsu FC, Harris TB et al (2009) The association of pericardial fat with incident coronary heart disease: the Multi-Ethnic Study of Atherosclerosis (MESA). Am J Clin Nutr 90(3):499–504

38. Silaghi A, Piercecchi-Marti MD, Grino M et al (2008) Epicardial adipose tissue extent: relationship with age, body fat distribution, and coronaropathy. Obesity (Silver Spring) 16(11):2424–2430

39. Perissinotto E, Pisent C, Sergi G, Grigoletto F (2002) Anthropometric measurements in the elderly: age and gender differences. Br J Nutr 87(2):177–186